

The Valence States of Nickel, Tin, and Sulfur in the Ternary Chalcogenide $\text{Ni}_3\text{Sn}_2\text{S}_2$ —XPS, ^{61}Ni and ^{119}Sn Mössbauer Investigations, and Band Structure Calculations**

Philipp Gütllich,* Klaus-Jürgen Range, Claudia Felser, Christian Schultz-Münzenberg, Wolfgang Tremel, Dorothee Walcher, and Markus Waldeck

$\text{Ni}_3\text{Sn}_2\text{S}_2$ is a ternary chalcogenide with a shandite structure (Figure 1).^[1] The shandite structure is an interesting structural variant which contains transition metals M (M = Co, Ni, Rh,

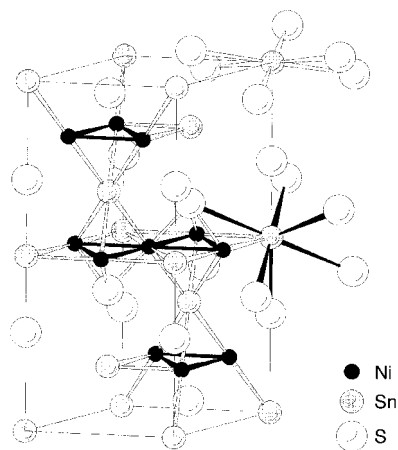


Figure 1. The crystal structure of $\text{Ni}_3\text{Sn}_2\text{S}_2$.

Pd), main group elements M' from Groups 3 and 4 ($M' = \text{In}$, Tl, Sn, Pb), as well as sulfur and/or selenium. The overall composition is $M_3M'_2X_2$, and there is no discernible phase width. There are bonding interactions between Ni and S (Ni–S 2.191 Å) as well as between Ni and Sn atoms (Ni–Sn(1) 2.730, Ni–Sn(2) 2.705 Å), in addition to metal–metal bonds between the Ni atoms (Ni–Ni 2.730 Å). In Ni metal the distance between two atoms is 2.50 Å. The three Ni atoms and one of the Sn atoms, Sn(2), form hexagonal-planar layers vertical to the c axis. Atom Sn(1) is surrounded by six Ni atoms in a trigonal-antiprismatic configuration. The S and Sn(1) atoms lie between the layers, whereby the Sn(2) atoms are surrounded in a hexagonal-planar manner by six Ni atoms; in the second coordination sphere there are six further S atoms in a distorted octahedral coordination environment. The third-order coordination environment contains three Sn(1) atoms in a pyramidal arrangement.

[*] Prof. Dr. P. Gütllich, Dr. C. Felser, Dr. C. Schultz-Münzenberg, Prof. Dr. W. Tremel, Dr. D. Walcher, Dipl.-Chem. M. Waldeck
Institut für Anorganische und Analytische Chemie der Universität
Staudinger Weg 9, D-55099 Mainz (Germany)
Fax: (+49) 6131-39-2990
E-mail: p.guetlich@uni-mainz.de
Prof. Dr. K.-J. Range
Institut für Anorganische Chemie der Universität
Universitätsstrasse 31, D-55099 Regensburg (Germany)

[**] This work was supported by the Deutsche Forschungsgemeinschaft, the Fonds der Chemischen Industrie, and the Materialwissenschaftliches Forschungszentrum der Universität Mainz.

Supporting information for this article is available on the WWW under <http://www.wiley-vch.de/home/angewandte/> or from the author.

Hitherto, the valence state of the contributing elements has been controversial. Assuming the presence of $\text{X}^{\text{II-}}$, four negative charges must be compensated. Preliminary investigations of $\text{Ni}_3\text{Sn}_2\text{S}_2$ by photoelectron spectroscopy (XPS) indicated the presence of three equivalent Ni atoms along with Sn^0 , which suggests the formulation $\text{Ni}_3^{1.33+}\text{Sn}_2^0\text{S}_2^{\text{II-}}$.^[2] This is in agreement with the appearance of a single crystallographic position for nickel. Judging the bonding situation on the basis of the interatomic distances does not lead to an unambiguous result. Thus, the sum of the atomic and ionic radii of Sn^0 and $\text{Sn}^{\text{II+}}$ (1.54 Å for the coordination number 12, 0.93 and 1.22 Å for the coordination numbers 6 and 8, respectively) for Sn(1)/Sn(2) and $\text{S}^{\text{II-}}$ yields Sn–S bond lengths of 3.06 and 2.77 Å, respectively. The experimentally determined Sn(1)–S bond lengths of 2.875 and 3.500 Å and Sn(2)–S bond lengths of 3.225 Å indicate that the valence state of tin cannot be unambiguously assigned on the basis of bond lengths and bond strengths. It is also partly dependent on the fact that the coordination numbers of Sn(1) and Sn(2) are not clearly defined because of the additional Ni neighbors. Moreover, an analysis of the Ni–S and Ni–Sn bond lengths only leads to the overall result that Ni–Sn interactions are probably important for the stability of $\text{Ni}_3\text{Sn}_2\text{S}_2$. A similar result was found from an estimation of the bonding relationships in $\text{Ni}_3\text{In}_2\text{S}_2$.

To clarify the question as to the valence states of nickel, tin, and sulfur in $\text{Ni}_3\text{Sn}_2\text{S}_2$, we have employed XPS as well as ^{61}Ni and ^{119}Sn Mössbauer spectroscopy. In addition, we have performed band structure calculations with the LMTO procedure (LMTO = linear muffin tin orbitals). The results are in agreement with those obtained experimentally.

The valence state of sulfur in $\text{Ni}_3\text{Sn}_2\text{S}_2$ was confirmed to be $\text{S}^{\text{II-}}$ by XPS. Figure 2 shows the photoelectron spectrum of the S2p signal (binding energy 162.8 eV). Also recorded are the

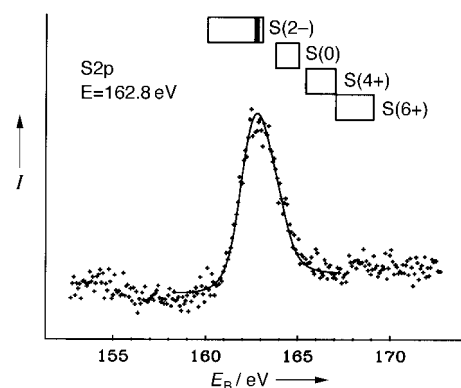


Figure 2. Photoelectron spectrum of $\text{Ni}_3\text{Sn}_2\text{S}_2$. E_B = binding energy.

expected regions for the binding energies of the species S^0 , S^{IV} , and S^{VI} .^[3] It can be seen that the assignment of the S2p signal to the $\text{S}^{\text{II-}}$ state is unambiguous. The measurement was performed on a ESCALAB-II apparatus (from VG). Non-monochromated $\text{MgK}\alpha$ radiation was used for the excitation. The calibration of the binding energy scale was based on the position of the C1s signal of aliphatic carbon at 285.0 eV. A corresponding XPS measurement of tin was not meaningful

because the position of the Sn3d signal for the states Sn^0 , Sn^{II} , and Sn^{IV} is almost identical (the difference is only about 0.3 eV).

In contrast, ^{119}Sn Mössbauer spectroscopy allowed the unambiguous assignment of tin to the divalent state. The room temperature ^{119}Sn Mössbauer spectrum is shown in Figure 3.

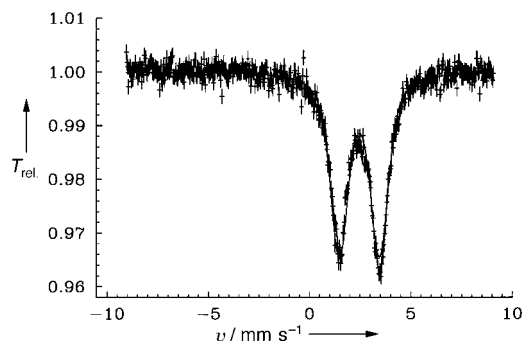


Figure 3. ^{119}Sn Mössbauer spectrum of $\text{Ni}_3\text{Sn}_2\text{S}_2$.

The spectrum, fitted to Lorentzian lines, gave an isomeric shift of $\delta = 2.48 \text{ mm s}^{-1}$ (relative to the source material BaSnO_3) and a quadrupole splitting of $\Delta E_Q = 1.89 \text{ mm s}^{-1}$. Both parameters are characteristic of Sn^{II} .^[4] The crystallographically different positions of Sn(1) and Sn(2) atoms are not noticeable in the Mössbauer spectrum.

The 67.4-keV transition of ^{61}Ni was used for the measurement of the ^{61}Ni Mössbauer spectrum.^[5] The Mössbauer source material was $(^{62}\text{Ni}/^{61}\text{Co})_{0.86}\text{Cr}_{0.14}$; this alloy does not usually cause any particular hyperfine interactions which would lead to a broadening of the linewidths. The short-lived mother nuclide ^{61}Co ($t_{1/2} = 99 \text{ min}$) was produced in the MAMI microtron at Mainz (Germany) by the nuclear reaction $^{62}\text{Ni}(\gamma, p)^{61}\text{Co}$ with bremsstrahlung of 20–25 MeV after slowing down the electrons with an energy of 850 MeV. A platelet ($\approx 4 \times 4 \text{ mm}^2$) of the ^{62}Ni -enriched alloy $^{62}\text{Ni}_{0.86}\text{Cr}_{0.14}$ was transported to the irradiation position through an approximately 50 m long rabbit system. After an irradiation time of about 2 h, the radioactive source material was pneumatically ejected and placed into a cryostat in which the sample to be measured as the Mössbauer absorber was already cooled to 4.2 K. The Mössbauer spectrum shown in Figure 4 was fitted to Lorentzian lines. The observed isomeric shift, $\delta = +0.04 \pm 0.02 \text{ mm s}^{-1}$, is in agreement with the valence

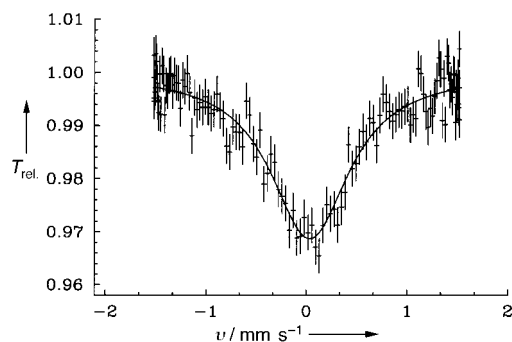


Figure 4. ^{61}Ni Mössbauer spectrum of $\text{Ni}_3\text{Sn}_2\text{S}_2$.

state Ni^0 .^[5] There was no significant observable increase in the linewidth as a result of magnetic hyperfine interactions.

The band structure of $\text{Ni}_3\text{Sn}_2\text{S}_2$ was self-consistently calculated within the framework of density functional theory^[6] by means of the TB-LMTO-ASA method (TB-LMTO-ASA = tight binding linear muffin tin orbitals atomic sphere approximation).^[7–10] To exclude the possibility that a magnetic ground state is energetically favored, the calculations were also performed with spin polarization in the local spin density approximation. The density of states was calculated by the tetrahedron method^[11, 12] with 1017 k points in the irreducible section of the Brillouin zone. The s, p, and d muffin-tin orbitals of Ni, S, and Sn were chosen for the basis set. The d muffin-tin orbitals of S and Sn were not completely included in the calculations in order to avoid “ghost bands”. The inner electrons were treated as a “soft core”. To avoid too large an overlap between the atomic spheres within the framework of the ASA, 15 empty spheres per unit cell were included and their optimum positions calculated from the Hartree potentials of the atoms with an automatic procedure.^[9] The respective COHP (crystal orbital Hamilton population)^[13] was used to investigate the bonding interactions, and the electron localization function (ELF)^[14] was used to find the localized orbitals.

To summarize the electronic properties of the compound, the total density of states (total DOS) and the partial density of states in $\text{Ni}_3\text{Sn}_2\text{S}_2$ are given in Figure 5. The compound is, as

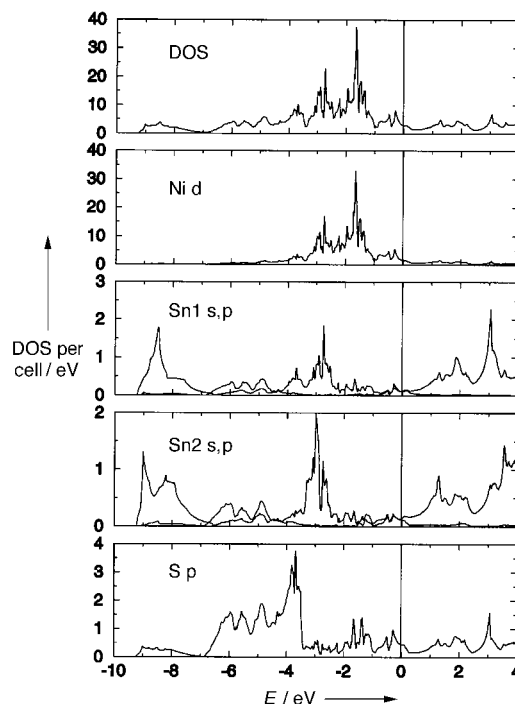


Figure 5. Density of states (DOS) of $\text{Ni}_3\text{Sn}_2\text{S}_2$.

expected, metallic (no valence-type construction, short metal–metal distances). The density of states at the Fermi level E_F amounts to 3.2 states per unit cell and eV, and is therefore relatively low so that a strong magnetic interaction can be excluded. Thus, the spin-polarization calculations also lead to

a paramagnetic ground state. The s states of the sulfur lie 14.5–13 eV below the Fermi level (not shown in Figure 5). The lower edge of the valence band at 9 eV below E_F is produced by s states of Sn(1) and Sn(2), which are separated by a “pseudogap” from the p states of sulfur, whose center lies 5 eV below the Fermi level. The occupation of the two s bands from Sn(1) and Sn(2) below the Fermi level leads to the conclusion that the valence state of Sn must be +2 or lower. Since both s bands show only a small dispersion and no eigenvector contribution from other orbitals, these bands must result from lone pairs of electrons.

The Ni d states determine the density of states just below the Fermi level, that is between –3.5 and –1 eV. Above E_F there is no significant contribution from the Ni d states. The Ni d bands are completely occupied, which confirms the valence state Ni^0 . Because of the Ni–Sn(1) interaction (shortest Ni–Sn distance) there are Sn(1) p states not only below E_F —however, only in the region of the Ni d states—but also above E_F .

Bonding interactions in complex structures can be most easily understood by means of the COHPs, the density of states weighted with the corresponding Hamilton matrix elements. The strongest bonding interaction, combined with the shortest interatomic distance, is the Ni–S interaction (Figure 6). In the region of the s and p states of sulfur this

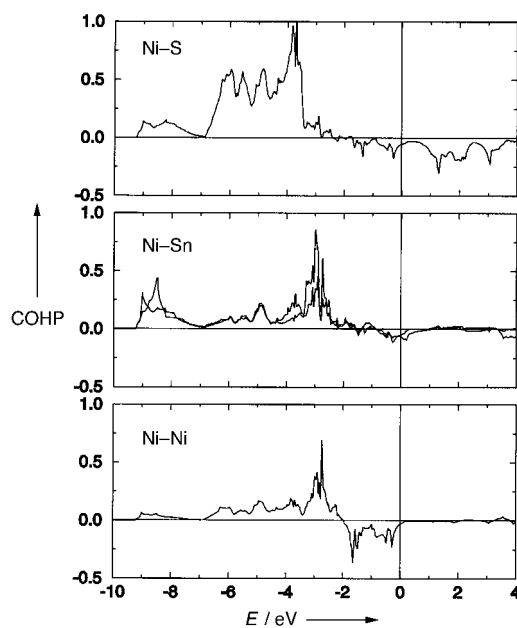


Figure 6. Crystal orbital Hamilton population (COHP) of $Ni_3Sn_2S_2$.

interaction is bonding (positive COHP values) and is already antibonding below the Fermi level in the region of the metal d states. In addition to the Ni d states, the s and p states which lie above E_F also contribute to the bonding interaction. Figure 6 shows that the center of the antibonding interaction lies above the Fermi level. Furthermore, the somewhat weaker Ni–Sn interaction is overall bonding. In the region of the Sn s and the Ni d states the interaction is bonding, and in the region of the Fermi level antibonding. Above the Fermi level, in the region where the Sn p states dominate, the interaction is, as expected, antibonding. The Ni–Ni interaction is overall nonbonding, since nearly all the d states are filled so that the bonding and

antibonding interactions cancel each other out. At the Fermi level the Ni–Ni interaction is nonbonding; however, about 3 eV above the Fermi level the metal–metal interaction is established by the s and p orbitals of Ni.

Figure 7a shows the ELF in the (010) plane, and Figure 7b the corresponding ELF in the (001) plane. The probability of finding an electron pair with opposing spins is normalized to 1,

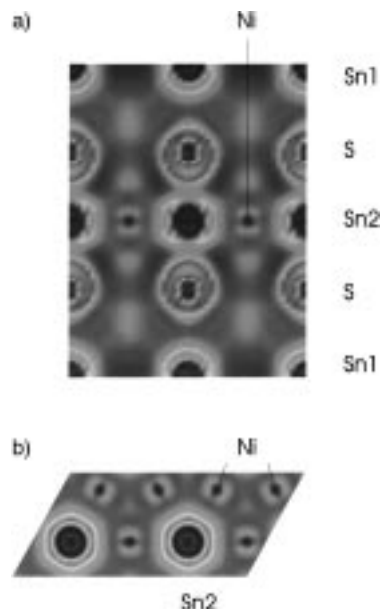


Figure 7. Electron localization function (ELF) of $Ni_3Sn_2S_2$ in the (010) plane (a) and in the (001) plane (b).

whereby high ELF values correspond to a value of 1 and thus to a high probability of finding paired electrons (light regions). The ELF has the value of 0.5 in a homogeneous electron gas. Regions which are avoided by electron pairs with opposing spins are represented darker. We have chosen the (010) plane, since this plane contains Sn(1), Sn(2), Ni, and S atoms.

High maxima around the sulfur atoms show that, in spite of the “covalency” of the bond between Ni and S (see the COHP diagram), the electron pairs are localized on the sulfur as a consequence of the difference in electronegativity. The lone electron pairs of the two crystallographically different Sn atoms have differing shapes. The electron pair of Sn(2) is localized around the atom with spherical symmetry. The electron pair of Sn(1) in the Ni–Sn plane is shaped to fit to the symmetry of the surrounding atoms: it forms a hexagon in the *a,b* plane (Figure 7b). The nickel atoms in the Ni–Sn(1) plane are in a trigonal arrangement. Even if the absolute values of the ELF at and between the Ni atoms are not high because of the d character of the valence electrons, it can still be recognized that the three-center, two-electron bonds between the three nickel atoms are also important in this compound. This is similar to the situation in $LiNbO_2$,^[15] TaS_2 , and GdI_2 .^[16]

The results presented here show that $Ni_3Sn_2S_2$ is a metal which is best described with the valence electron configuration $(Ni^0)_3(Sn(1)^{II})(Sn(2)^{II})(S^{II-})_2$.

Received: January 28, 1999 [Z12973IE]
German version: *Angew. Chem.* **1999**, *111*, 2524–2527

Keywords: density functional calculations • Moessbauer spectroscopy • photoelectron spectroscopy • solid-state structures

- [1] M. Zabel, S. Wandinger, K.-J. Range, *Z. Naturforsch. B* **1979**, *34*, 238.
- [2] K.-J. Range, personal communication.
- [3] D. Briggs, M. P. Seak, *Practical Surface Analysis*, Salle-Sauerländer, Frankfurt am Main, **1990**.
- [4] N. Greenwood, T. C. Gibb, *Mössbauer Spectroscopy*, Chapman and Hall, London, **1971**.
- [5] P. Gülich, R. Link, A. Trautwein, *Mössbauer Spectroscopy and Transition Metal Chemistry*, Spinger, Berlin, **1978**, p. 113.
- [6] U. von Barth, L. Hedin, *J. Phys. C* **1971**, 2064.
- [7] a) O. K. Andersen, O. Jepsen, *Phys. Rev. Lett.* **1984**, *53*, 2571; b) O. K. Andersen, Z. Pawłowska, O. Jepsen, *Phys. Rev. B* **1986**, *34*, 5253.
- [8] O. K. Andersen, O. Jepsen, D. Glözel in *Highlights of Condensed-Matter Theory* (Eds.: F. Bassani, F. Fumi, M. P. Tosi), North-Holland, New York, **1985**.
- [9] O. K. Andersen, *Phys. Rev. B* **1975**, *12*, 3060.
- [10] H. L. Skriver, *The LMTO Method*, Springer, Berlin, **1984**.
- [11] O. Jepsen, O. K. Andersen, *Solid State Commun.* **1971**, *9*, 1763.
- [12] O. Jepsen, O. K. Andersen, *Z. Phys. B* **1995**, *97*, 35.
- [13] F. Boucher, O. Jepsen, O. K. Andersen, unpublished results; R. Dronskowski, P. Blöchl, *J. Phys. Chem.*, **1993**, *97*, 8619.
- [14] a) A. Savin, O. Jepsen, H. J. Flad, O. K. Andersen, H. W. Preuss, H. G. von Schnering, *Angew. Chem.* **1992**, *104*, 187; b) *Angew. Chem. Int. Ed. Engl.* **1992**, *31*, 187.
- [15] C. Felser, K. Thiem, R. Seshadri, *J. Mater. Chem.*, in press.
- [16] C. Felser, K. Ahn, R. K. Kremer, R. Seshadri, A. Simon, *J. Solid. State Chem.*, submitted.

Samarium-Mediated β -Elimination in Dihalo Alcohols: Diastereoselective Synthesis of (Z)-Vinyl Halides**

José M. Concellón,* Pablo L. Bernad, and Juan A. Pérez-Andrés


Diastereoselective formation of carbon–carbon double bonds has received considerable attention in organic chemistry.^[1] Among many other methods, the 1,2-elimination reaction is a powerful route to alkenes.^[2] Usually, the alkene obtained in these processes is isolated as a *Z/E* mixture, and only the use of starting materials with defined stereochemistry affords single diastereoisomers.^[3] Vinyl halides^[4] are syntheti-

cally even more interesting, since they readily undergo carbon–carbon bond formation.^[5] Some years ago we reported a useful process for the synthesis of vinyl chlorides and bromides by lithium-promoted β -elimination in 1,1-dihalo-2-silyloxyalkanes, but this reaction took place with poor diastereoselectivity.^[6] Zinc was also used, but again no diastereoselectivity was achieved.^[7]

In recent years we have used samarium diiodide as an alternative to traditional organometallic compounds^[8] and have described iodo-^[9a] and diiodomethylations^[9b] of carbonyl compounds with this reagent. We considered the possibility of using samarium diiodide to promote a β -elimination reaction in 1,1-dihaloalkane-2-ols. The use of SmI_2 in reductive elimination reactions has not been studied as widely as other transformations. Only β -hydroxy- or β -acetoxysulfones have received some attention, providing the thermodynamically favored (*E*)-olefin.^[10] The treatment of epoxides with samarium diiodide and various additives gave mixtures of *Z* and *E* diastereoisomers.^[11]

Here we describe our studies on diastereoselective 1,2-elimination in O-acetylated 1,1-dihaloalkane-2-ols with samarium diiodide. Our first trials were carried out with 1,1-diiodononane-2-ol (prepared by reaction of octanal with $\text{SmI}_2/\text{CHI}_3$ ^[9b] or diiodomethylithium^[12]) as a model substrate. When this alcohol was added to a solution of SmI_2 in THF, vinyl iodide **2a** was obtained in high yield but with very poor diastereoselectivity.^[13] A similar result was obtained with O-silylated 1,1-diiodononane-2-ol. However, when O-acetylated 1,1-diiodononane-2-ol was used, (*Z*)-1-iodonon-1-ene^[14] was obtained with high diastereoselectivity (Table 1).^[15] Transformation was complete after a few minutes at room temperature. The usual diastereoselectivity/temperature trend was not observed; instead, increasing the temperature enhanced the diastereoselectivity (Table 1, entries 1–3).^[16] Solvent effects were also studied: addition of *N,N'*-dimethyl-*N,N'*-propylene urea (DMPU) as co-solvent to the solution of SmI_2 in THF leads to lower diastereoselectivity (entry 4); when the


Table 1. Diastereoselective SmI_2 -mediated β -elimination reaction of O-acetyl diiodo alcohols.

					
Entry	1	R	T [°C]	<i>Z/E</i> ^[a]	Yield [%] ^[b]
1	1a	C ₇ H ₁₅	50	94/6	88
2	1a	C ₇ H ₁₅	20	92/8	86
3	1a	C ₇ H ₁₅	–20	89/11	88
4	1a	C ₇ H ₁₅	20 ^[c]	62/38	72
5	1a	C ₇ H ₁₅	55 ^[d]	84/16	40
6	1b	Cyclohexyl	50	94/6	64
7	1c	MeCH(Ph)	50	94/6	83
8	1d ^[e]	Me ₂ C=CHCH ₂ CH ₂ CH(Me)CH ₂	50	94/6	70
9	1e ^[e]	(<i>S</i>)-MeCH(OBn)	50	87/13	75
10	1f ^[f]	C ₆ H ₁₃ CH(Cl)	50	93/7	77
11	1g	Ph	50	72/28	92
12	1h	MeCH=CH	50	83/17	— ^[g]
13	1h	MeCH=CH	20	71/29	— ^[g]

[a] Determined on crude reaction products by ¹H NMR spectroscopy and/or GC-MS. [b] Yield of isolated products. [c] With addition of DMPU. [d] With acetonitrile as solvent. [e] A 1/1 mixture of diastereoisomers. [f] A 3/1 mixture of diastereoisomers. [g] This compound decomposed on purification.

[*] Dr. J. M. Concellón, Dr. P. L. Bernad, J. A. Pérez-Andrés
Departamento de Química Orgánica e Inorgánica
Facultad de Química, Universidad de Oviedo
E-33071 Oviedo (Spain)
Fax: (+34) 98-510-34-46
E-mail: jmcg@sauron.quimica.uniovi.es

[**] We thank II Plan Regional de Investigación del Principado de Asturias (PBP-PG197-01) and Ministerio de Educación y Ciencia (PB97-1278) for financial support. J.M.C. thanks Carmen Fernández for her help.

 Supporting information for this article is available on the WWW under <http://www.wiley-vch.de/home/angewandte/> or from the author.